DE GRUYTER Z. Phys. Chem. 2017; 231(7–8): 1443–1453

C. Vinod Chandran*, Kai Volgmann, Suliman Nakhal, Reinhard Uecker, Elena Witt, Martin Lerch and Paul Heitjans*

Local Ion Dynamics in Polycrystalline β-$LiGaO_2$: A Solid-State NMR Study

DOI 10.1515/zpch-2016-0920
Received October 21, 2016; accepted March 17, 2017

Abstract: Solid-state nuclear magnetic resonance spectroscopy is an efficient technique to characterize dynamics and structure of materials. It has been widely used to elucidate ion dynamics in lithium ion conductors. Fast moving lithium ions are needed in energy storage devices, whereas slow ion motion is exploited in some materials used, for example, as blankets in fusion reactors. β-lithium gallium oxide ($LiGaO_2$) is a slow Li^+ ionic conductor similar to γ-lithium aluminum oxide ($LiAlO_2$). In an ion conductor, in addition to the main diffusion process, localized motions (to-and-fro jumps) may be present. In the present work, with the help of solid-state NMR experiments, we report on the localized movements of Li^+ ionic species in β-$LiGaO_2$ in the temperature range between 300 K and 450 K. In this work, we have mainly extracted the peculiarities of ion dynamics from ^{7}Li spin-alignment echo NMR measurements and the observation of the motional narrowing of the central transition signal of ^{7}Li.

Keywords: β-$LiGaO_2$; ^{71}Ga NMR; ^{7}Li NMR; Li ion diffusion; motional narrowing; solid-state NMR; spin-alignment echo.

1 Introduction

Lithium containing solid materials have several applications mainly based on the mobility of the Li ions within these systems. Lithiated solids with highly mobile

***Corresponding authors: C. Vinod Chandran and Paul Heitjans,** Institut für Physikalische Chemie und Elektrochemie, Leibniz Universität Hannover, Callinstr. 3-3a, 30167 Hannover, Germany; and Zentrum für Festkörperchemie und Neue Materialien (ZFM), Leibniz Universität Hannover, Callinstr. 3-3a, 30167 Hannover, Germany, e-mail: vinod.nair@pci.uni-hannover.de (C.V. Chandran), heitjans@pci.uni-hannover.de (P. Heitjans)
Kai Volgmann and Elena Witt: Institut für Physikalische Chemie und Elektrochemie, Leibniz Universität Hannover, Callinstr. 3-3a, 30167 Hannover, Germany; and Zentrum für Festkörperchemie und Neue Materialien (ZFM), Leibniz Universität Hannover, Callinstr. 3-3a, 30167 Hannover, Germany
Suliman Nakhal and Martin Lerch: Technische Universität Berlin, Strasse des 17. Juni 135, 10623 Berlin, Germany
Reinhard Uecker: Leibniz-Institut für Kristallzüchtung, Max-Born-Strasse 2, 12489 Berlin, Germany

Li ions have been used as efficient lithium ion battery (LIB) materials for decades [1–3]. But the materials with slow Li ion diffusion (e.g. lithium aluminate) are also employed, for example as tritium-breeder blankets for fusion reactors [4, 5], or as substrates for semiconductor growth [6]. The fundamental dynamic processes in slow ion conductors have much less been studied and are not yet fully understood. In such materials, in addition to the main slow ionic diffusion mode, there may be faster localized motions present. These localized (or to-and-fro) jumps of ions are usually difficult to observe with regular mobility or conductivity investigations. In the present study, we employed nuclear magnetic resonance (NMR) spectroscopy to monitor local ionic jumps, in which only a small part of the Li ions are involved.

There are several reports on solid-state NMR studies of materials with fast diffusing Li ions [7–11]. Most of them focus on materials used in LIB's and investigate their dynamics, structure and conductivity behaviors. But there are only a few reports available on NMR studies of materials with purely slow Li dynamic modes alone [12–14]. Witt et al. [13] studied the slow ionic diffusion in microcrystalline (*m*-) γ-lithium aluminate ($LiAlO_2$). From variable-temperature spin-lattice relaxation (SLR) studies [15], spin-alignment echo (SAE) experiments [16] and conductivity measurements [17], a slow overall ionic diffusion with a diffusion coefficient of the order of 10^{-19} m^2s^{-1} at 473 K and an activation energy of 0.7 eV were found. In addition, the Li^+ motion led to the averaging of dipolar broadening of the central transition ^7Li signal of *m*-$LiAlO_2$. This motional narrowing ocurred in the temperature range between 500 and 900 K. The full-width at half-maximum (FWHM) decreased from 7 kHz to a few hundreds of Hz in this temperature range [13]. A reduction of FWHM of this order is usual for a complete motional narrowing process (involving all Li ions) leaving behind only the inhomogeneous line broadening. Recently, a substantial increase of ionic mobility has been observed on reduction of particle size in $LiAlO_2$ by mechanical milling [18].

$LiGaO_2$ is an interesting material, in which structural differences contribute significantly towards ionic conductivity. The high-pressure phase α-$LiGaO_2$ [19] forms layered solid solutions with $LiCoO_2$ [20], α-$LiAlO_2$ [21], and $LiNi_{1-x}Co_xO_2$ [22], which can be employed as potential electrode materials for Li-ion batteries. However, an ultra-slow Li ionic diffusion is expected for polycrystalline β-$LiGaO_2$ similar to γ-$LiAlO_2$, despite their structural differences. But to probe such slow dynamics, the NMR experiments have to be carried out at very high-temperatures. However, localized motions can be probed at lower temperatures. In the present work, we report localized Li ion motion based on our observations of motional narrowing (between 293 and 473 K) and SAE experiments (between 373 and 448 K) carried out in polycrystalline (*ss*-) β-$LiGaO_2$ which was prepared using

a solid-state synthesis route. A comparison to a powdered single crystal of (*cr*-) β-$LiGaO_2$ is also presented in the case of the SAE experiments.

2 Experimental

2.1 Materials

2.1.1 Solid-state synthesis of β-$LiGaO_2$

Microcrystalline β-$LiGaO_2$ powder was prepared by reacting an appropriate mixture of Li_2CO_3 (99.997 %, Aldrich) and Ga_2O_3 (99.99 %, Aldrich) in a closed corundum crucible. After homogenizing the powders and pressing them to pellets, the samples were slowly heated up to 673 K and annealed for 1 h. This was followed by two additional heating steps at 873 K (10 h) and 1103 K (4 h). Finally, the pellets were quenched to ambient temperature by removing the pellets out of the furnace. Phase purity and the presence of the desired polymorph were confirmed by X-ray powder diffraction (PANalytical XPert PRO MPD, Cu-Kα radiation). The pellets were ground in an argon glove-box to produce the sample (*ss*-$LiGaO_2$) used for the NMR experiments. The polycrystalline *ss*-$LiGaO_2$ sample has an average particle size of 5 μm.

2.1.2 Growth of β-$LiGaO_2$ bulk crystals

β-$LiGaO_2$ bulk crystals were grown using the conventional Czochralski technique with RF-heating and automatic diameter control. The starting materials Li_2CO_3 and Ga_2O_3 were of 99.99% purity. Both powders were dried, mixed in the stoichiometric ratio, sintered, pressed following standard procedures, and finally molten in a 40 mL crucible. $LiGaO_2$ melts congruently at about 1585 °C. This high melting temperature requires the use of an iridium crucible. To decrease the melt evaporation, the temperature gradients in the growth set-up were adjusted by an active after-heater also consisting of iridium. The crystals were pulled along the *a*-axis with a rate of 1 mm/h and a rotation rate of 15 rpm, and the growth atmosphere consisted of flowing nitrogen. The achieved single crystals were of about 60 mm in length and 15 mm in diameter. These crystals were finely ground using mortar and pestle in an argon glove-box to get the polycrystalline sample (*cr*-$LiGaO_2$) for the NMR experiments. The polycrystalline *cr*-$LiGaO_2$ sample has an average particle size of 100 μm.

2.2 Solid-state NMR

The solid-state NMR experiments were carried out using a Bruker Avance III 600 spectrometer, at a magnetic field strength of 14 T, corresponding to Larmor frequencies of 233.30 MHz and 183.07 MHz for ^{7}Li and ^{71}Ga, respectively. A 5 mm single-resonance probe has been used for static NMR measurements and a 2.5 mm double-resonance probe for magic-angle spinning (MAS) experiments. For static ^{7}Li experiments a standard solid-echo sequence has been used. For high-resolution MAS spectra, the samples were spun at 20 kHz frequency. A very small tip angle of $\pi/16$ was used for ^{7}Li and ^{71}Ga NMR. For all samples, the T_1 time was determined using saturation recovery experiments and recycle delays of $5 \times T_1$ were used. For *cr*-$LiGaO_2$, the SAE experiments were done with a starting saturation pulse train. The recycle delay used for ^{7}Li NMR experiments for *ss*-$LiGaO_2$ was of the order of tens of seconds. The ^{7}Li and ^{71}Ga NMR spectra were referenced (0 ppm) against dilute solutions of LiCl and $Ga(NO_3)_3$, respectively. The ^{7}Li SAE decays were observed under static conditions with the standard Jeener-Broekaert pulse sequence [23]. The preparation time (τ_p) of 15 μs was kept constant and the mixing time (t_{mix}) was varied from 100 μs to 100 s. The ^{1}H dipolar decoupling experiments were carried out with the robust frequency-swept SPINAL sequence [24, 25] with a radio-frquency strength of 150 kHz. All static variable-temperature NMR experiments were done on samples sealed in glass tubes and under dry nitrogen flow conditions.

3 Results and discussion

3.1 ^{71}Ga and ^{7}Li NMR spectroscopy

β-$LiGaO_2$ crystallizes in a distorted wurtzite type orthorhombic structure with a space group $Pna2_1$ at ambient conditions [26]. The structure consists of LiO_4 and GaO_4 tetrahedra. Since there is only one crystallographic Ga site, this is reflected in the Ga NMR spectrum. Gallium has two naturally abundant NMR active isotopes, ^{69}Ga (60.108%) and ^{71}Ga (39.892%). Both the nuclei possess a quadrupole moment, as their spin number ($I = 3/2$) exceeds 1/2. The interaction of the nuclear quadrupole moment with the electric field gradient (EFG) in the electronic surroundings of the nucleus is called the quadrupolar interaction. The magnitude of the quadrupolar interaction is measured using the quadrupolar coupling constant (Q_{CC}). The quadrupolar coupling constant can be defined as

$$Q_{CC} = \frac{V_{zz} eQ}{h} \tag{1}$$

where V_{zz} is the largest component of the EFG tensor V, eQ is the quadrupole moment and h is the Planck constant. The asymmetry of the tensor V is represented by the parameter η_Q,

$$\eta_Q = \frac{V_{xx} - V_{yy}}{V_{zz}} \tag{2}$$

The dependence of Q_{CC} and η_Q on the symmetry of the electronic surroundings helps to determine atomic coordination behaviors in structural studies. The magnetogyric ratio of ^{71}Ga (8.18×10^7 rad T^{-1} s^{-1}) is bigger than that of ^{69}Ga (6.44×10^7 rad T^{-1} s^{-1}). The quadrupole moment of ^{69}Ga (17.1 fm^2) is larger than that of ^{71}Ga (10.7 fm^2), resulting in broader signals for ^{69}Ga. Therefore, among these two nuclei, ^{71}Ga gives more resolved NMR signals, and can hence be used, for example, to confirm the absence of any significant impurity phase. ^{71}Ga NMR of both β-$LiGaO_2$ [27] and γ-$LiGaO_2$ (atmospheric pressure modification of α-$LiGaO_2$) [21] have been reported in literature. Figure 1a and b show the experimental central-transition ^{71}Ga spectra of *ss*-$LiGaO_2$ and *cr*-$LiGaO_2$, respectively. A single ^{71}Ga signal is observed for both the samples. The central-transition signals in both cases are broadened by the second-order quadrupolar interaction. Figure 1c shows a simulation of the

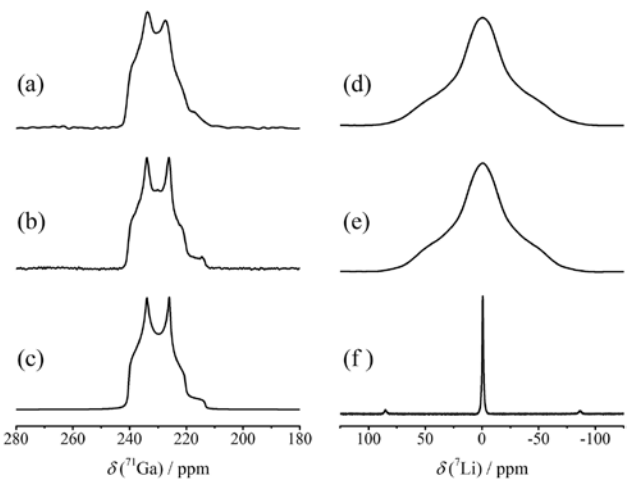

Fig. 1: On the left are the central transition ^{71}Ga NMR spectra of (a) *ss*-$LiGaO_2$ and (b) *cr*-$LiGaO_2$ under sample spinning (MAS) at a frequency of 20 kHz and (c) simulated line-shape using $\delta_{iso} = 241$ ppm, $Q_{CC} = 3.8$ MHz and $\eta_Q = 0.4$. On the right are the static ^{7}Li NMR solid-echo spectra of (d) *ss*-$LiGaO_2$, (e) *cr*-$LiGaO_2$ and (f) the magic-angle spinning (at frequency of 20 kHz) spectrum of *ss*-$LiGaO_2$.

spectrum with the characteristic NMR parameters, such as Q_{CC} of 3.8 MHz, η_Q of 0.4 and isotropic chemical shift (δ_{iso}) of 241 ppm. These values are in very good agreement with the values for β-$LiGaO_2$ reported in literature [27]. The main difference between the ^{71}Ga NMR spectra of *ss*-$LiGaO_2$ and *cr*-$LiGaO_2$ is the rounding of the edges and steps of the second-order quadrupole pattern of the central-transition signal in the case of *ss*-$LiGaO_2$. This is mainly due to the large surface and increased number of defects in the sample prepared by solid-state synthesis, which induce distributions to NMR interactions, like chemical shielding, quadrupole coupling and/or dipolar coupling.

Solid-echo ^{7}Li NMR experiments carried out on *ss*-$LiGaO_2$ and *cr*-$LiGaO_2$ resulted in central (narrow contribution) as well as satellite (broad contribution) transition signals as shown in Figure 1d and e. The quadrupole coupling constant calculated from the largest splitting steps is 42 kHz in both the cases, assuming $\eta_Q = 0$. The first-order quadrupole interactions get partially averaged with sample spinning at a frequency of 20 kHz, and the isotropic central transition and the remnant spinning-side bands can be seen for *ss*-$LiGaO_2$ in Figure 1f. The ^{7}Li MAS NMR spectrum of *cr*-$LiGaO_2$ (not shown) is similar to that of *ss*-$LiGaO_2$.

3.2 ^{7}Li NMR motional narrowing

The solid-echo ^{7}Li NMR spectrum of *ss*-$LiGaO_2$ shows a central transition signal, which is broadened mainly by Li-Li dipolar interactions. The FWHM of this signal changes slightly with temperature. Generally the FWHM has a high value at a lower temperature at the rigid lattice limit, and on complete averaging of dipolar interactions at high temperatures, it reaches the extreme narrowing limit. However, also in the present case, the reduction in FWHM with temperature can be the resultant of a dynamic process. The line-width changes from 6.3 kHz to 5.4 kHz within the measurement temperature range (293–473 K). This is shown in Figure 2, together with a blown-up image (inset) with a solid-line to guide the eye. A complete motional averaging due to the full averaging of the dipolar interaction would decrease the FWHM drastically by at least one order of magnitude (like from a few kHz to a few hundreds of Hz, as in the case of $LiAlO_2$ [13]). But in the present study, the line-width reduction is only showing a change of a few hundreds of kHz. This is ascribed to a partial averaging of dipolar interactions by the effect of a localized dynamic process, in which a subgroup of the Li ions are involved. A similar dynamic process has been observed in the past for $Li_{15}Si_4$ while probing ^{7}Li motional narrowing phenomena [28], and it has been attributed to limited Li diffusion due to geometrical restrictions. Localized motions usually represent to-and-fro jump processes between an ionic site and a vacancy or an interstitial.

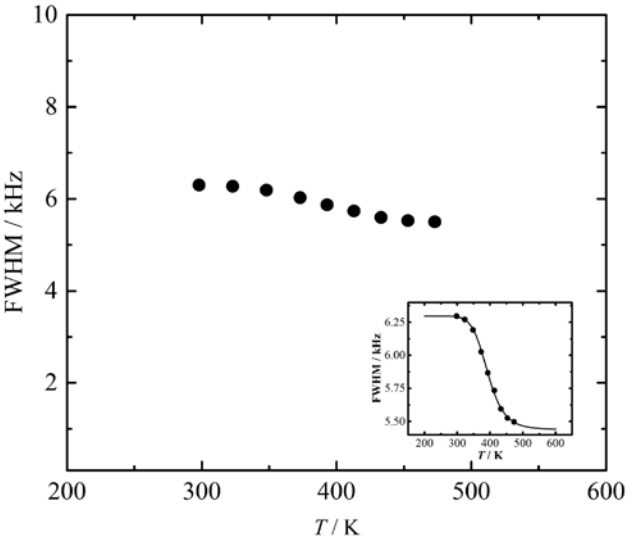

Fig. 2: The full-width at half-maximum of the central transition of static ^{7}Li NMR spectra of *ss*-$LiGaO_2$ plotted against the measurement temperature showing the motional narrowing corresponding to localized motion of Li ions. A blown-up image is shown on the inset with a solid-line to guide the eye.

But in the present case, the number of Li ions participating in the whole process is significantly small. Only approximately $1 \pm 0.5\%$ of the total number of Li ions are involved in the localized dynamics, as estimated from the fraction of the NMR signal representing the mobile species. For these experiments, recording of fully relaxed ^{7}Li solid-echo spectra are necessary. For *ss*-$LiGaO_2$, exhibiting ^{7}Li T_1 times of a few seconds, these variable-temperature experiments were possible, unlike in the case of *cr*-$LiGaO_2$ with T_1 times of the order of thousands of seconds. The large difference in T_1 times of the two samples is a resultant of two orders of difference in particle size, and the increased defect concentration in the sample prepared using solid-state synthesis. The absence of H-related impurities in $LiGaO_2$ was confirmed with ^{1}H NMR. In addition ^{1}H-decoupling experiments were carried out during the ^{7}Li solid-echo experiments. No differences in ^{7}Li line-widths or intensities were observed in experiments with and without ^{1}H decoupling.

3.3 ^{7}Li spin-alignment echo

To study the localized motion on a different time scale, we have employed ^{7}Li SAE NMR experiments. Slow diffusion of ionic species can be investigated with SAE

experiments, as shown in several previous reports [13, 29–31]. The advantage of the method is in the fact that direct estimation of ionic jump rates are possible from single-temperature measurements, which is not the case in relaxation measurements. This is carried out with the help of a two-dimensional array of SAE experiments with mixing-time dependence. The resultant echo amplitudes are plotted as a function of the mixing time (t_{mix}), as shown in Figure 3, for *ss*-$LiGaO_2$ at 373–448 K. The jump rates (τ_{SAE}^{-1}) are extracted from the curves using stretched exponential functions. The stretching exponents (γ) were 0.49, 0.50, 0.50 and 0.49 at 373, 398, 423 and 448 K, respectively. It is seen from the estimated jump rates that their magnitudes did not change significantly over the applied temperature range. But the same temperature range was influential in the ionic motion observed in the motional narrowing experiments. Therefore, the small changes in ionic jump rates are realistic in these conditions and they belong to the localized ion dynamics process.

Figure 4 shows the temperature dependence of the ionic jump rates in an Arrhenius plot and a linear fit is applied. The slope of the linear fit provides the Arrhenius activation energy (E_A) from the SAE experiments. In the case of *ss*-$LiGaO_2$, the estimated E_A is 0.13 eV, which is smaller compared to activation barriers in other Li-containing solids. This small magnitude of E_A is also indicating the presence of a localized motion in the $LiGaO_2$ system. The extraction of diffusion coefficients are not desirable for such short to-and-fro jump processes, as they do not contribute to large scale translational diffusion. Since the ^{7}Li T_1 time is relatively smaller for *ss*-$LiGaO_2$, the SAE experiments at higher temperatures were done in acceptable experiment times. For *cr*-$LiGaO_2$, however, the SAE pulse program

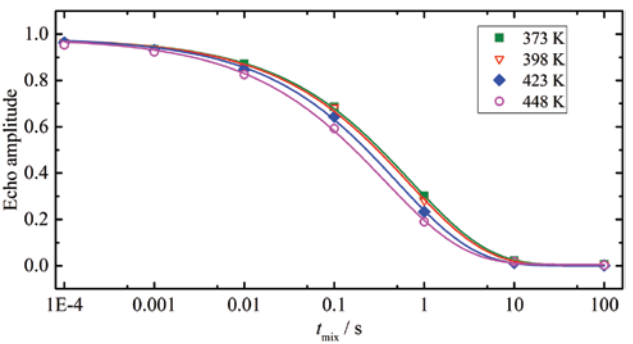

Fig. 3: Mixing-time (t_{mix}) dependence of the ^{7}Li spin-alignment echo NMR amplitudes of *ss*-$LiGaO_2$ at temperatures from 373 K to 448 K. The stretched exponential fits yielded the correlation times (τ_{SAE}) for different temperatures, where the stretching coefficients (γ) remained close to 0.5.

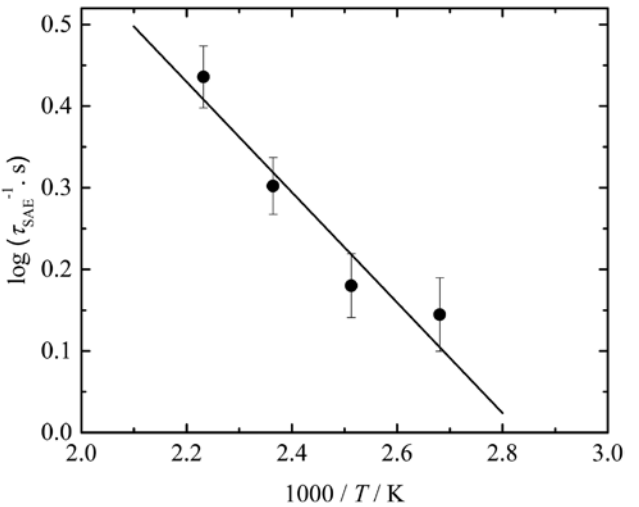

Fig. 4: The Arrhenius plot showing the dependence of ^{7}Li τ_{SAE}^{-1} of Li ions in *ss*-$LiGaO_2$ with inverse temperature. The linear fit yielded an activation energy of 0.13 eV, corresponding to a localized Li motion in $LiGaO_2$.

had to be modified to include saturation pulse train to shorten the duration of the experiments. The temperature dependent SAE jump rates in this case were fitted with a linear function which showed a higher Arrhenius activation energy (0.40 eV). However, the E_A for overall ionic diffusion in $LiGaO_2$ is expected to have similar magnitudes as that for $LiAlO_2$ (i.e. 0.7 eV). This might also indicate the presence of a localized motion in $LiGaO_2$ involving only a small number of Li ions.

4 Conclusions

Solid-state NMR spectroscopy methods have been employed to elucidate the localized Li ionic motion in polycrystalline $LiGaO_2$. ^{7}Li motional narrowing of the central transition signal indicated a partially averaged Li-Li dipolar interaction pointing to local ionic motion in the temperature range between 300 K and 450 K. In addition, ^{7}Li SAE experiments showed ionic jump rates between 10^0 and 10^1 s^{-1} (at 373 – 448 K) with a very small activation energy (0.13 eV) for $LiGaO_2$, indicating a to-and-fro jump motion process.

Acknowledgements: The authors would like to express their gratitude for the financial support by Graduiertenkolleg Energiespeicher und Elektromobilität

Niedersachsen (GEENI) and DFG Research Unit 1277 Mobilität von Lithium-Ionen in Festkörpern (molife).

References

1. M. S. Whittingham, Chem. Rev. **104** (2004) 4271.
2. J. B. Goodenough, Y. Kim, Chem. Mater. **22** (2010) 587.
3. N. Nitta, F. Wu, J. T. Lee, G. Yushin, Mater. Today **18** (2015) 252.
4. N. Roux, S. Tanaka, C. Johnson, R. Verall, Fusion Engin. Design **41** (1998) 31.
5. J. G. van der Laan, H. Kawamura, N. Roux, D. Yamaki, J. Nucl. Mater. **283 – 287** (2000) 99.
6. P. Waltereit, O. Brandt, K. H. Ploog, Appl. Phys. Lett. **75** (1999) 2029.
7. A. Kuhn, P. Sreeraj, R. Pöttgen, H.-D. Wiemhöfer, M. Wilkening, P. Heitjans, J. Am. Chem. Soc. **133** (2011) 11018.
8. D. Blanchard, A. Nale, D. Sveinbjörnsson, T. M. Eggenhuisen, M. H. W. Verkuijlen, Suwarno, T. Vegge, A. P. M. Kentgens, P. E. de Jongh, Adv. Funct. Mater. **25** (2015) 184.
9. C. V. Chandran, P. Heitjans, Annu. Rep. Nucl. Magn. Reson. Spectrosc. **89** (2016) 1.
10. C. V. Chandran, S. Pristat, E. Witt, F. Tietz, P. Heitjans, J. Phys. Chem. C **120** (2016) 8436.
11. K. Bösebeck, C. V. Chandran, B. K. Licht, M. Binnewies, P. Heitjans, Energy Technol. **12** (2016) 1598.
12. B. Ruprecht, M. Wilkening, R. Uecker, P. Heitjans, Phys. Chem. Chem. Phys. **14** (2012) 11974.
13. E. Witt, S. Nakhal, C. V. Chandran, M. Lerch, P. Heitjans, Z. Phys. Chem. **229** (2015) 1327.
14. D. Wiedemann, S. Nakhal, J. Rahn, E. Witt, M. M. Islam, S. Zander, P. Heitjans, H. Schmidt, T. Bredow, M. Wilkening, M. Lerch, Chem. Mater. **28** (2016) 915.
15. P. Heitjans, A. Schirmer, S. Indris, In: Diffusion in Condensed Matter – Methods, Materials, Models, P. Heitjans, J. Kärger (Eds.), Springer, Berlin (2005).
16. R. Boehmer, K. R. Jeffrey, M. Vogel, Prog. Nucl. Magn. Reson. **50** (2007) 87.
17. K. Funke, C. Cramer, D. Wilmer, In: Diffusion in Condensed Matter – Methods, Materials, Models, P. Heitjans, J. Kärger (Eds.), Springer, Berlin (2005).
18. D. Wohlmuth, V. Epp, P. Bottke, B. Bitschnau, I. Letofsky-Papst, M. Kriechbaum, H. Amenitsch, F. Hofer, M. Wilkening, I. Hanzu, J. Mater. Chem. A **2** (2014) 20295.
19. M. Marezio, J. P. Remeika, J. Phys. Chem. Solids **26** (1965) 1277.
20. R. Stoyanova, E. Zhecheva, G. Bromiley, T. B. Ballaran, R. Alcántara, J.-I. Corredor, J.-L. Tirado, J. Mater. Chem. **12** (2002) 2501.
21. E. Zhecheva, R. Stoyanova, R. Alcántara, J. L. Tirado, J. Phys. Chem. B **107** (2003) 4290.
22. R. Stoyanova, E. Zhecheva, R. Alcántara, J.-L. Tirado, G. Bromiley, F. Bromiley, T. B. Ballaran, J. Mater. Chem. **14** (2004) 366.
23. J. Jeener, P. Broekaert, Phys. Rev. **157** (1967) 232.
24. C. V. Chandran, T. Bräuniger, J. Magn. Reson. 200 (2009) 226.
25. C. V. Chandran, G. Hempel, T. Bräuniger, Solid State Nucl. Magn. Reson. 40 (2011) 84.
26. G. M. Kuz'micheva, V. B. Rybakov, A. V. Gaister, E. V. Zharikov, Inorg. Mater. (USSR) **37** (2001) 281.
27. J. T. Ash, P. J. Grandinetti, Magn. Reson. Chem. **44** (2006) 823.

28. S. Dupke, T. Langer, R. Pöttgen, M. Winter, S. Passerini, H. Eckert, Phys. Chem. Chem. Phys. **14** (2012) 6496.
29. M. Wilkening, W. Küchler, P. Heitjans, Phys. Rev. Lett. **97** (2006) 065901.
30. M. Wilkening, P. Heitjans, J. Phys. Condens. Mater. **18** (2006) 9849.
31. M. Wilkening, A. Kuhn, P. Heitjans, Phys. Rev. B **78** (2008) 054303.